Robust *Ab Initio* Predictions for Nuclear Rotational Structure in the Be Isotopes

M. A. Caprio[a], P. J. Fasano[a], J. P. Vary[b], P. Maris[b] and J. Hartley[a,c,*]

[a] *Department of Physics, University of Notre Dame, Notre Dame, Indiana 46556, USA*
[b] *Department of Physics and Astronomy, Iowa State University, Ames, Iowa 50011, USA*
[c] *Department of Chemistry and Physics, Erskine College, Due West, South Carolina 29639, USA*

Abstract

No-core configuration interaction (NCCI) calculations for p-shell nuclei give rise to rotational bands, identified by strong intraband $E2$ transitions and by rotational patterns for excitation energies, electromagnetic moments, and electromagnetic transitions. However, convergence rates differ significantly for different rotational observables and for different rotational bands. The choice of internucleon interaction may also substantially impact the convergence rates. Consequently, there is a substantial gap between simply observing the *qualitative* emergence of rotation in *ab initio* calculations and actually carrying out detailed *quantitative* comparisons. In this contribution, we illustrate the convergence properties of rotational band energy parameters extracted from NCCI calculations, and compare these predictions with experiment, for the isotopes $^{7-11}$Be, and for the JISP16 and Daejeon16 interactions.

Keywords: *Nuclear rotation; no-core configuration interaction (NCCI); Be isotopes*

1 Introduction

Ab initio nuclear theory aims to describe nuclei, with quantitative precision, from the underlying internucleon interactions. Light nuclei are known to display rotational band structure (see, e. g., Refs. [1–4]). Therefore, we should at least aspire for *ab initio* theory to be able to predict rotational band structure. However, there are challenges to obtaining converged calculations of the relevant observables, both energies and electromagnetic transition strengths [5–8].

There are thus a few basic questions to be asked about the emergence of rotation in *ab initio* calculations of light nuclei:

*Present address: Department of Physics and Astronomy, Michigan State University, East Lansing, MI 48824, USA.

Proceedings of the International Conference 'Nuclear Theory in the Supercomputing Era — 2018' (NTSE-2018), Daejeon, South Korea, October 29 – November 2, 2018, eds. A. M. Shirokov and A. I. Mazur. Pacific National University, Khabarovsk, Russia, 2019, p. 250.

http://www.ntse.khb.ru/files/uploads/2018/proceedings/Caprio.pdf.

(1) Is there a *qualitative emergence* of rotational "features" in the calculated results? These features include rotational energy patterns and transition patterns.

(2) Can robust *quantitative predictions* be made for rotational observables? These observables include rotational band energy parameters or intrinsic matrix elements. Here we must have good convergence of the results of the many-body calculation, at which point we can then explore the robustness of the predictions across possible internucleon interactions.

(3) Once the *ab initio* description for nuclear rotation is solidly established, what can it tell us about the structure of these rotational states? This understanding may come in the form of identifying, e. g., many-body symmetries [9–12] or cluster structure [2, 4, 13] underlying the rotation.

Regarding the first, qualitative question, no-core configuration interaction (NCCI) [14] calculations for p-shell nuclei give rise to rotational bands, identified by strong intraband $E2$ transitions and by rotational patterns for excitation energies, electromagnetic moments, and electromagnetic transitions [15, 16] (see also Ref. [17] for a pedagogical review). However, convergence rates differ significantly for different rotational observables and for different rotational bands, as well as in calculations based on different internucleon interactions [17]. Consequently, there is a substantial gap between simply observing the *qualitative* emergence of rotation in *ab initio* calculations and actually obtaining detailed *quantitative* predictions for comparison with experiment.

In this contribution, we focus on quantitative predictions of rotational band energy parameters. We first illustrate the convergence properties of rotational parameters extracted from NCCI calculations, taking ^{11}Be as an example (Section 2). We then obtain *ab initio* predictions for rotational band parameters across the isotopes $^{7-11}$Be. We explore the robustness of these predictions with respect to the choice of internucleon interaction (JISP16 [18] and Daejeon16 [19]) and compare these predictions with experiment (Section 3).

2 Illustration: Rotational bands in ^{11}Be

2.1 Excitation spectrum and bands

To illustrate the nature of the rotational bands obtained in NCCI calculations, let us take ^{11}Be as an example. In this nucleus, we encounter bands with qualitatively different termination and convergence properties.

A calculated eigenvalue spectrum for ^{11}Be is shown in Fig. 1.[1] The detailed results depend upon the particular choice of the internucleon interaction (here, JISP16 [18] plus Coulomb interaction between protons) and truncated space (here, up to $N_{\max} = 8$ excitation quanta, and with oscillator basis length scale given by $\hbar\omega = 20\,\mathrm{MeV}$), as we shall explore in subsequent Sections, but the example calculation in Fig. 1 provide a representative illustration of the general rotational features.

Band members are expected to have energies following the rotational formula $E(J) = E_0 + AJ(J+1)$, where the rotational energy constant $A \equiv \hbar^2/(2\mathcal{J})$ is inversely related to the moment of inertia $\mathcal{J}$ of the rotational intrinsic state, and the intercept parameter $E_0 = E_K - AK^2$ is related to the energy E_K of the rotational

[1] The NCCI calculations shown here are obtained using the code MFDn [20–22].

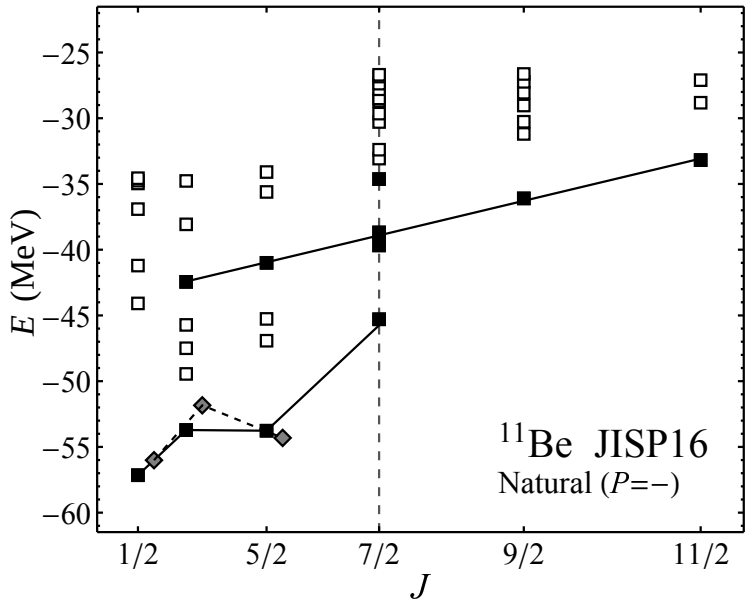

Figure 1: Calculated energy eigenvalues (squares) for states in the natural (negative) parity space of ^{11}Be, with the JISP16 interaction; the three lowest calculated unnatural (positive) parity states are also shown (diamonds, displaced horizontally for clarity). Energies are plotted with respect to angular momenta scaled as $J(J+1)$. Solid symbols indicate band members, as identified by strong $E2$ transitions and other supporting observables. Lines indicate rotational fits (1) to the calculated energies of the band members. Calculated with $N_{\max} = 8$ (or $N_{\max} = 9$ for unnatural parity) at $\hbar\omega = 20$ MeV.

intrinsic state [23, 24].[2] The level energies in Fig. 1 are therefore plotted against angular momenta scaled as $J(J+1)$, so that the energies within a band follow a linear pattern. For $K = 1/2$ bands, the Coriolis contribution to the kinetic energy significantly modifies this pattern, yielding an energy staggering which is given, in first-order perturbation theory, by

$$E(J) = E_0 + A\big[J(J+1) + a(-)^{J+1/2}(J+\tfrac{1}{2})\big], \tag{1}$$

where the Coriolis decoupling parameter a depends upon the structure of the rotational intrinsic state.

Rotational band members are shown in Fig. 1 by filled symbols. These identifications are based not simply on the level energies, but rather on strong $E2$ connections (for illustration, see Figs. 6, 10, and 14 of Ref. [17]).

The lowest filling of harmonic oscillator shells possible for ^{11}Be, consistent with Pauli exclusion, has an odd number of nucleons in the negative-parity p shell. Thus, the "natural" parity for ^{11}Be, as would be obtained in a traditional $0\hbar\omega$ shell model description or an $N_{\max} = 0$ NCCI calculation, is negative. In Fig. 1, we focus on the

[2] Under the assumption of axial symmetry, each band is characterized by a projection K of the angular momentum on the intrinsic symmetry axis, and the rotational band members have angular momenta $J \geq K$.

natural (negative) parity states (indicated by squares) and show only the lowest three "unnatural" (positive) parity states for comparison (diamonds).

In this particular calculation (Fig. 1), the lowest positive parity state ($1/2^+$) lies slightly above the lowest negative parity state ($1/2^-$). However, experimentally, the ground state of ^{11}Be is $1/2^+$, lying 0.320 MeV below a $1/2^-$ excited state [25]. (Such a reversal of the ground state parity relative to the natural parity is known as *parity inversion*.) Different rates of convergence between the natural and unnatural parity states makes it challenging to predict the level ordering when the separation of energies is so small.

The lowest negative-parity band has $K^P = 1/2^-$ and apparently terminates with the $7/2^-$ state. This angular momentum $J = 7/2$ (indicated by the dashed vertical line in Fig. 1) is the highest which can be obtained in a p-shell description of ^{11}Be, that is, in the shell model $0\hbar\omega$ valence space or in an NCCI $N_{\max} = 0$ calculation.

On the other hand, the excited negative-parity $K^P = 3/2^-$ band extends past the maximal valence angular momentum. The $J \leq 7/2$ band members lie in a region of the excitation spectrum with a comparatively high level density and are thus subject to mixing with the "background" non-rotational states. Such mixing occurs when an approximate accidental degeneracy of the rotational state and background states leads to a small energy denominator for mixing. Since we found that the energies of these states converge differently with $N_{\max}$ and $\hbar\omega$, mixing for any given rotational state might arise in one truncated calculation but not the next. For instance, in the particular calculation shown here, the $E2$ strengths suggest that the excited $7/2^-$ band member is actually fragmented over three states, as indicated by the filled symbols. Starting with $J = 9/2$, this band becomes yrast, and the band members are comparatively well-isolated.

The lowest calculated positive parity states are the $1/2^+$, $3/2^+$, and $5/2^+$ members of a $K^P = 1/2^+$ band. This band continues to much higher angular momentum than shown here, as may be seen in Fig. 3(e) of Ref. [16].

2.2 Dependence of the calculated bands on $N_{\max}$ truncation

While Fig. 1 illustrates the qualitative features of the rotational patterns which arise in NCCI calculations, it represents an approximate calculation of the spectrum, as obtained in a truncated space. It is thus only an unconverged "snapshot", along the path towards the true results which would be obtained if the many-body problem could be solved in the full, untruncated many-body space.

To see how the rotational pattern evolves, as we progress through calculations truncated to successively higher numbers of oscillator excitations, let us focus on the rotational band members in the negative parity space of ^{11}Be. We trace out the energies obtained for $N_{\max} = 6$, 8, and 10 in Fig. 2 (top). These energies are far from converged. Each level moves downward by several MeV for each step in $N_{\max}$.

However, the energies of levels within a band move downward nearly in lockstep. Thus, if we look instead at *excitation* energies, as in Fig. 2 (bottom), here taken relative to the lowest ($1/2^-$) negative parity state, the energies of the $K^P = 1/2^-$ band members are comparatively stable. In fact, only the excitation energy of the terminating $7/2^-$ band member changes noticeably at an MeV scale.

The $K^P = 3/2^-$ band is still converging downward relative to the $K^P = 1/2^-$

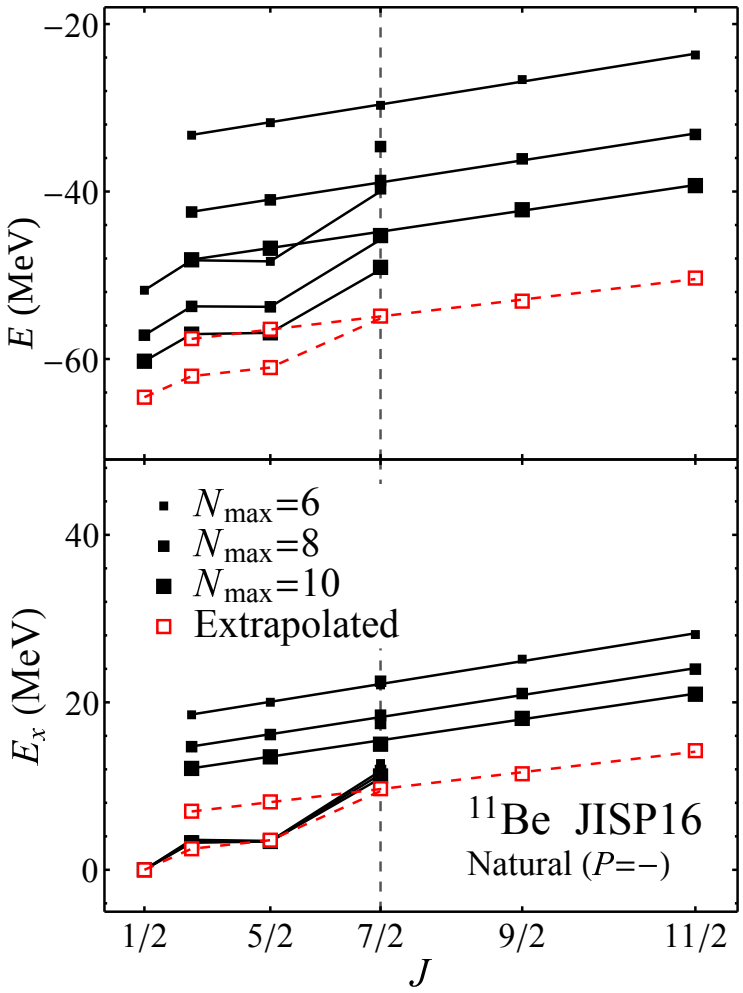

Figure 2: Convergence of calculated energy eigenvalues (top) and excitation energies (bottom) with $N_{\max}$, for rotational band members in the natural (negative) parity space of ^{11}Be. Successively larger symbols indicate successively higher $N_{\max}$ values ($N_{\max} = 6$, 8, and 10). The open symbols indicate exponentially extrapolated level energies. Lines indicate rotational fits (1) to the calculated (or extrapolated) energies of these band members. Calculated with the JISP16 interaction at $\hbar\omega = 20\,\mathrm{MeV}$.

band with increasing $N_{\max}$, reflected in the decreasing excitation energies in Fig. 2 (bottom). It is not obvious where we could expect these excitation energies to settle, if we could solve the nuclear many-body problem in the full, untruncated space.

However, we can attempt to *estimate* the full-space result by assuming a functional form for the convergence of the calculated energy eigenvalues. For instance, the sequence of eigenvalues computed at successive $N_{\max}$ appears to follow a roughly geometric convergence pattern, suggestive of a decaying exponential in $N_{\max}$ [6,26,27]:

$$E(N_{\max}) = c_0 + c_1 \exp(-c_2 N_{\max}). \tag{2}$$

Since calculated energies at three $N_{\max}$ values are required to fix the three parameters in Eq. (2), this functional form provides a three-point extrapolation formula for energies, giving the estimate $E \to c_0$ as $N_{\max} \to \infty$. This is only an *ad hoc* phenomenological prescription, but it provides an idea of what might be plausible for the full-space results.

Extrapolated energies for the ^{11}Be band members are shown in Fig. 2 (open symbols): as eigenvalues (top), and then as excitation energies, taken relative to the extrapolated $1/2^-$ eigenvalue (bottom). While the extrapolated energies of the $K^P = 3/2^-$ band members still lie above those of the $K^P = 1/2^-$ band at lower angular momenta, the lower slope of the excited band, combined with the Coriolis staggering of the $K^P = 1/2^-$ band members, leads to nearly degenerate extrapolated energies for the $7/2^-$ members of these two bands. If such a degeneracy were to arise, we could expect significant two-state mixing to occur between the two rotational configurations in the $7/2^-$ band members (similar to the mixing of the excited $7/2^-$ with the background states seen already at higher excitation energy, in Fig. 1). The level repulsion induced by this mixing would be highly non-perturbative and would thus frustrate any simple attempt at extrapolating the energies from low-$N_{\max}$ calculations where the mixing is not yet in effect.

2.3 Stability of calculated rotational energy parameters

Rotational energy parameters extracted from calculations for the ^{11}Be bands are examined, as functions of $N_{\max}$ and $\hbar\omega$ and for different interactions, in Figs. 3–5. There are several questions to be answered for these extracted parameter values:

(1) Are the calculated values stable against the parameters $N_{\max}$ and $\hbar\omega$ of the truncated space?

(2) If so, are the predictions consistent across the different internucleon interactions?

(3) How do these predictions then compare to experiment?

Recall that these parameters are the inertial (or slope) parameter A, energy (or intercept) parameter E_0, and Coriolis decoupling (or staggering) parameter a (for $K = 1/2$). The excitation energy E_x of bands relative to each other is then measured by the difference in their band energy parameters E_0 (we use the $K^P = 1/2^-$ band as our reference for excitation energies).[3]

It is instructive to examine and compare the convergence behaviors of the parameters A, a, and E_x for the various bands, and subject to different interactions. Successive curves in each plot in Figs. 3–5 represent calculations at successively higher $N_{\max}$, obtained for different oscillator basis length scales given by $\hbar\omega$.[4] Each

[3]Translating differences of band energy parameters into differences in intrinsic excitation energies would require that we also take into account the correction $\propto K^2$ (Section 2.1).

[4]These rotational parameters are extracted from the energies of the "cleanest" band members, least subject to mixing with nearby states. Thus, the parameters for the $K^P = 1/2^-$ band in Fig. 3 are extracted from the three lowest-energy band members ($1/2^-$, $3/2^-$, and $5/2^-$), and similarly for the $K^P = 1/2^+$ band in Fig. 5. On the other hand, for the $K^P = 3/2^-$ band, the lower-energy band members are in a region of higher level density and subject to mixing with background states, which can perturb their energies and make it more difficult to trace their evolution across calculations with different $N_{\max}$ and $\hbar\omega$. Therefore, we take energy parameters defined by a straight line through the $9/2^-$ and $11/2^-$ band members for the analysis in Fig. 4 (the rotational fit lines in Figs. 1 and 2 were instead obtained as a combined fit to the $3/2^-$, $5/2^-$, $9/2^-$ and $11/2^-$ band members).

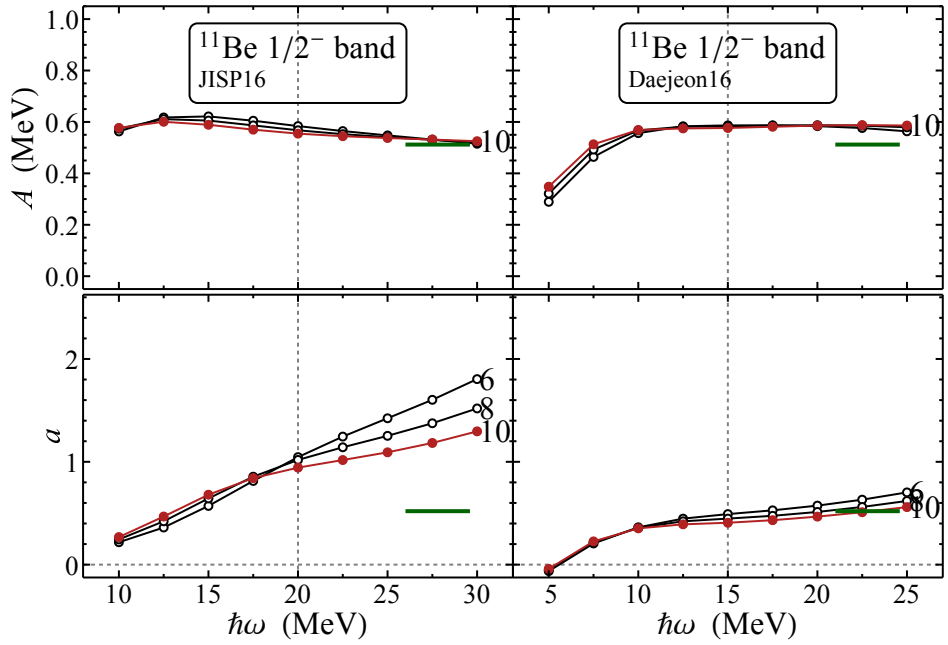

Figure 3: Dependence of the extracted rotational energy parameters, for the $K^P = 1/2^-$ band of ^{11}Be, on the truncation parameters $N_{\max}$ and $\hbar\omega$ of the NCCI space in which the calculations are carried out. Successive curves are for successively higher $N_{\max}$ values ($N_{\max} = 6$, 8, and 10, noted alongside curve). Experimental values (horizontal lines) are shown for comparison ($A = 0.51$ MeV and $a = 0.52$). The vertical dashed lines indicate the approximate location of the variational energy minimum, in $\hbar\omega$, of the calculated ground state energy (see text).

figure then includes results based on the JISP16 (left) and Daejeon16 (right) interactions.[5] The $\hbar\omega$ range is centered on the approximate location of the variational energy minimum for the computed ground state energy, which occurs at $\hbar\omega \approx 20$ MeV for JISP16 and $\hbar\omega \approx 15$ MeV for Daejeon16 (vertical dotted lines). Experimental values for the rotational band parameters [29], extracted from the observed level energies, are shown for comparison (horizontal lines).[6]

[5]The JISP16 interaction [18] is a two-body interaction derived from nucleon-nucleon scattering data by J-matrix inverse scattering, then adjusted via a phase-shift equivalent transformations to better describe light nuclei with $A \leq 16$. The Daejeon16 interaction [19] is instead obtained from the Entem–Machleidt (EM) N^{3}LO chiral interaction [28], softened via a similarity renormalization group (SRG) transformation to enhance convergence, and then likewise adjusted via a phase-shift equivalent transformation to better describe light nuclei with $A \leq 16$.

[6] The experimental band parameter values for the bands in ^{11}Be are based on fits of the rotational energy formula to the experimental levels, as summarized in Table III of Ref. [29]: for the $1/2^-$ band, the $1/2^-$ at 0.320 MeV, $3/2^-$ at 2.654 MeV, and $5/2^-$ at 3.889 MeV; for the $3/2^-$ band, the $3/2^-$ at 3.955 MeV and $5/2^-$ at 5.255 MeV; for the $1/2^+$ band, the $1/2^+$ ground state, $3/2^+$ at 3.400 MeV, and $5/2^+$ at 1.783 MeV. These assignments of levels to bands in ^{11}Be follow Refs. [3, 30], while energies are from Ref. [25]. However, there are conflicting spin-parity assignments in the literature. For instance, the level at 3.4 MeV was assigned as $3/2^-$ in (t, p) [31], $(3/2^-)$ in β decay [32], and $(3/2, 5/2)^+$ in breakup [33], and is evaluated as $(3/2^-, 3/2^+)$ [25]. The level at 3.9 MeV, was assigned as $3/2^+$ in (t, p) [31] but as $5/2^-$ in β decay [32], corroborated as negative parity in transfer reactions [34], and evaluated as $5/2^-$ [25].

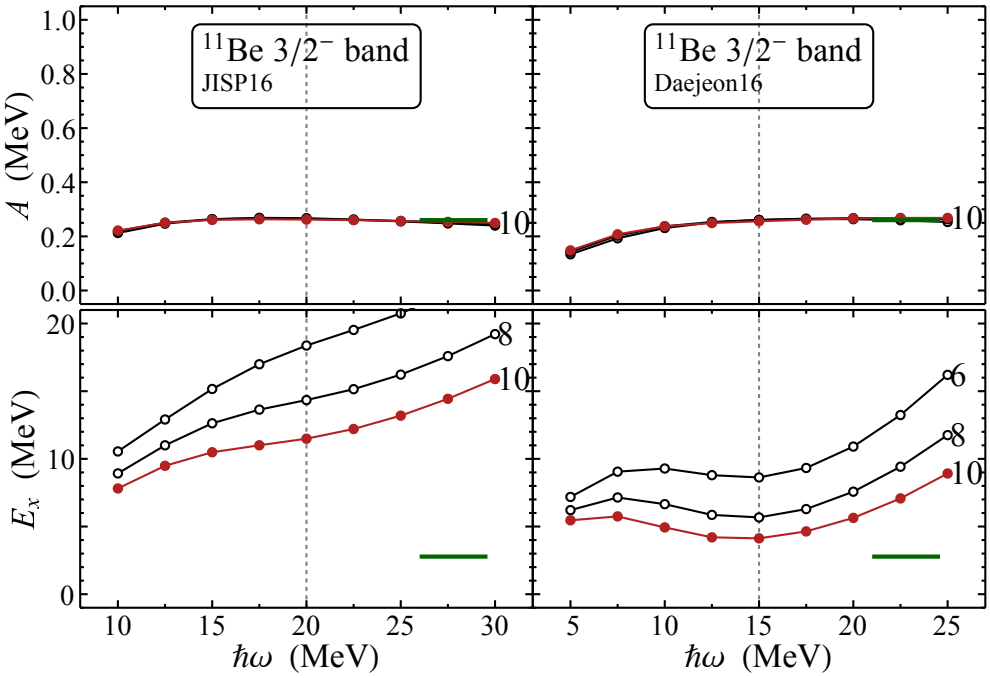

Figure 4: Dependence of the extracted rotational energy parameters, for the excited $K^P = 3/2^-$ band of ^{11}Be, on the truncation parameters $N_{\max}$ and $\hbar\omega$ of the NCCI space in which the calculations are carried out. Successive curves are for successively higher $N_{\max}$ values ($N_{\max} = 6$, 8, and 10, noted alongside curve). The band excitation energy E_x is taken relative to the $K^P = 1/2^-$ band. Experimental values (horizontal lines) are shown for comparison ($A = 0.26\,\mathrm{MeV}$ and $E_x = 2.77\,\mathrm{MeV}$). The vertical dashed lines indicate the approximate location of the variational energy minimum, in $\hbar\omega$, of the calculated ground state energy (see text).

The slope parameter A follows entirely from relative energies within a band, which were already seen from Figs. 1 and 2 to be comparatively well-converged. From the top panels in Figs. 3–5, the calculated A parameter is essentially converged for the Daejeon16 calculations (in the vicinity of the variational minimum $\hbar\omega$), while there is still some residual dependence on $N_{\max}$ (at the few-percent level) and $\hbar\omega$ for the JISP16 calculations. There is remarkable consistency across these two interactions, as well as with the experimental values. A shallower slope corresponds in the rotational picture to a larger moment of inertia. Note that the excited $K^P = 3/2^-$ band, by this measure, has a moment of inertia roughly twice that of the $K^P = 1/2^-$ band, both in calculations and experiment (this greater moment of inertia may be understood in terms of α cluster structure and the molecular orbitals occupied by the neutrons [13]).

Even though the Coriolis decoupling parameter a [Figs. 3 (bottom) and 5 (middle)] is likewise determined only from relative energies within a band, it is found to be much more sensitive to the truncation of the calculation. (This parameter is extracted essentially as a second difference in level energies, and numerical second derivatives are known to be sensitive to uncertainties or fluctuations in the inputs.) For instance, in the JISP16 calculations for the $K^P = 1/2^-$ band [Fig. 3 (bottom,left)], although

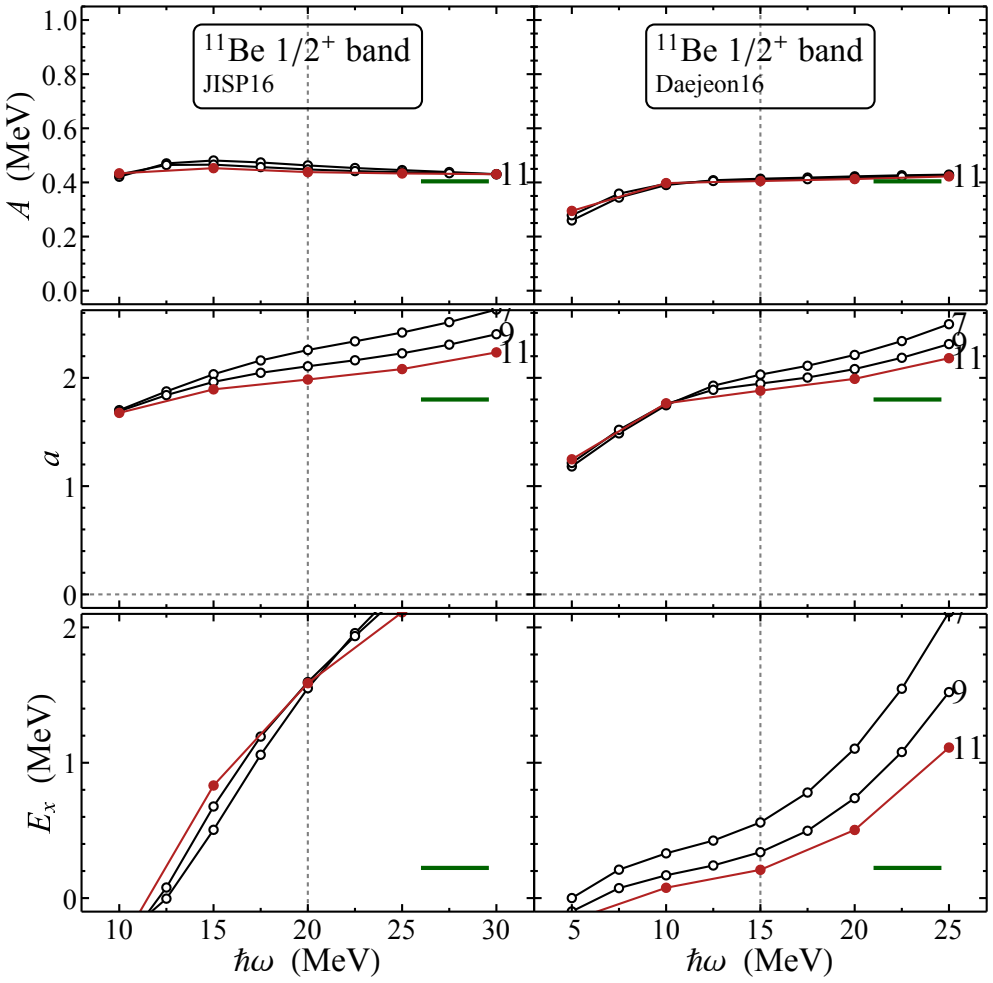

Figure 5: Dependence of the extracted rotational energy parameters, for the unnatural-parity $K^P = 1/2^+$ band of ^{11}Be, on the truncation parameters $N_{\max}$ and $\hbar\omega$ of the NCCI space in which the calculations are carried out. Successive curves are for successively higher $N_{\max}$ values ($N_{\max} = 7$, 9, and 11, noted alongside curve). The band excitation energy E_x is taken relative to the $K^P = 1/2^-$ band. Experimental values (horizontal lines) are shown for comparison ($A = 0.40$ MeV, $a = 1.80$, and $E_x = 0.22$ MeV). The vertical dashed lines indicate the approximate location of the variational energy minimum, in $\hbar\omega$, of the calculated ground state energy (see text).

the Coriolis decoupling parameter is deceptively independent of $N_{\max}$ at $\hbar\omega = 20$ MeV (vertical dashed line), there is still a strong $\hbar\omega$ dependence, which means that it is not yet possible to extract a converged value. On the other hand, a seems to be comparatively well converged in the Daejeon16 calculations for this same band [Fig. 3 (bottom,right)] and in close agreement with experiment ($a \approx 0.5$). For the $K^P = 1/2^+$ band, although the a parameter obtained for both interactions is developing a plateau (or shoulder) as a function of $\hbar\omega$, indicative of convergence [Fig. 5 (middle)], there is

still $N_{\max}$ dependence at about the 10% level. The calculated values are consistent with the much larger decoupling parameter ($a \approx 1.8$) experimentally found for this band.

Finally, the excitation energy of the $K^P = 3/2^-$ band [Figs. 4 (bottom)] is poorly converged, as already found in Section 2.2. The excitation energy of the unnatural parity $K^P = 1/2^+$ band [Figs. 5 (bottom)] is still highly $\hbar\omega$-dependent (though again deceptively $N_{\max}$ independent at $\hbar\omega = 20\,\mathrm{MeV}$) for the JISP16 interaction, while the excitation energy obtained in the Daejeon16 calculation is approaching convergence at the $\sim$0.1–0.2 MeV level and appears consistent with experiment. More detailed comparisons must rely upon extrapolation, as considered in the following discussion of band parameters along the Be isotopic chain (Section 3).

3 Rotational energy parameters for the Be isotopes

A variety of rotational bands were identified across the Be isotopes in Ref. [16]. These include examples of "short" bands (terminating at the maximal valence angular momentum) and "long" (non-terminating) bands, as well as unnatural parity bands, akin to those discussed above for ^{11}Be (Section 2).

We survey the rotational energy parameters extracted from *ab initio* calculations in Fig. 6. While the calculations in Ref. [16] made use of the JISP16 interaction without Coulomb contribution, and thus could not be directly compared to experiment, the present JISP16 and Daejeon16 calculations include Coulomb interaction and thus may be directly compared to experiment, convergence permitting. We do not attempt to display the sensitivity of the extracted parameters to the basis parameter $\hbar\omega$, but rather confine ourselves to the values obtained at the approximate variational energy minimum in $\hbar\omega$. However, we do show the sequence of extracted values for four successive $N_{\max}$ truncations, as a more limited indicator of convergence. We also show the band parameters obtained from exponentially extrapolated energies.

The first notable feature of the predicted band parameters in Fig. 6 is the overall global consistency between predictions with the JISP16 and Daejeon16 interactions, across the set of bands considered. Despite the caveat that significant remaining $\hbar\omega$-dependence of some of the extracted band parameters leaves their converged values in doubt (see Section 2.3), the values for both the A and a parameters obtained at the variational minimum in $\hbar\omega$ are generally largely $N_{\max}$-independent at the MeV scale considered here. In contrast, relative excitation energies of different bands are poorly converged, but even here the extrapolated energies are largely consistent across interactions.

The overall pattern of rotational band parameters closely matches experiment. Where discrepancies arise, the tendency is for the *ab initio* calculations to be consistent with each other rather than with experiment. Here it should be noted that there can be significant ambiguities in identification of the experimental band members (see, e. g., footnote 6), as well as fundamental uncertainties in comparing energies obtained in a bound-state formalism, such as NCCI, with those from experimental resonant scattering analysis.

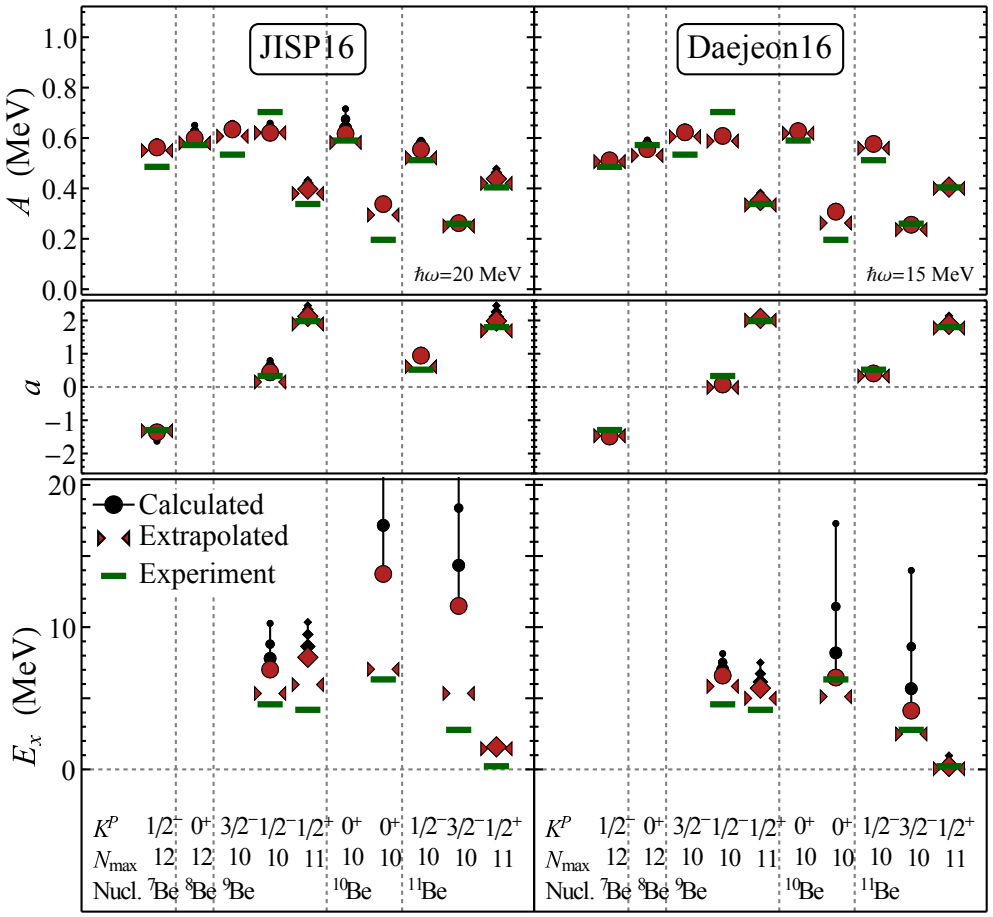

Figure 6: Band energy parameters for $^{7\text{–}11}$Be, extracted from calculated energy eigenvalues: rotational constant A (top), Coriolis decoupling parameter a (middle), and band excitation energy E_x (bottom), for the JISP16 (left) and Daejeon16 (right) internucleon interactions. Successively larger symbols indicate successively higher $N_{\max}$ values. Parameter values are also shown based on exponentially extrapolated level energies (paired triangles). Experimental values for the band energy parameters (horizontal lines) are shown for comparison [29]. The nuclide, band (K^P), and highest $N_{\max}$ value calculated are noted at the bottom of the plot. Results are obtained from calculations at $\hbar\omega = 20\,\text{MeV}$ for JISP16 and $\hbar\omega = 15\,\text{MeV}$ for Daejeon16.

4 Conclusion

We have explored the dependences of rotational band energy parameters on the truncation parameters of an oscillator-basis NCCI calculation for the illustrative case of ^{11}Be (Figs. 3–5) and, more generally, across the Be isotopes (Fig. 6). We find that *ab initio* calculations can provide quantitatively robust predictions for rotational band energy parameters in light (p-shell) nuclei. Even subject to the present limitations on *ab initio* many-body calculations, numerically robust predictions can be made for

rotational band parameters in the Be isotopes. The results obtained with two interactions of significantly different pedigree (the JISP16 interaction from J-matrix inverse scattering and the Daejeon16 interaction originating from chiral perturbation theory) yield highly consistent results. These results are also, overall, remarkably consistent with the experimentally observed band parameters.

Acknowledgements

We thank Jie Chen, Jakub Herko, and Anna McCoy for comments on the manuscript. This material is based upon work supported by the U.S. Department of Energy, Office of Science, under Award Numbers DE-FG02-95ER-40934, DESC00018223 (SciDAC/NUCLEI), and DE-FG02-87ER40371, and by the U.S. National Science Foundation under Award Number NSF-PHY05-52843. This research used computational resources of the University of Notre Dame Center for Research Computing and of the National Energy Research Scientific Computing Center (NERSC), a U.S. Department of Energy, Office of Science, user facility supported under Contract DE-AC02-05CH11231.

References

[1] J. D. Rogers, Annu. Rev. Nucl. Sci. **15**, 241 (1965).

[2] W. von Oertzen, Z. Phys. A **354**, 37 (1996).

[3] W. von Oertzen, Z. Phys. A **357**, 355 (1997).

[4] M. Freer, Rep. Prog. Phys. **70**, 2149 (2007).

[5] M. Pervin, S. C. Pieper and R. B. Wiringa, Phys. Rev. C **76**, 064319 (2007).

[6] S. K. Bogner, R. J. Furnstahl, P. Maris, R. J. Perry, A. Schwenk and J. Vary, Nucl. Phys. A **801**, 21 (2008).

[7] C. Cockrell, J. P. Vary and P. Maris, Phys. Rev. C **86**, 034325 (2012).

[8] P. Maris and J. P. Vary, Int. J. Mod. Phys. E **22**, 1330016 (2013).

[9] T. Dytrych, K. D. Sviratcheva, C. Bahri, J. P. Draayer, and J. P. Vary, Phys. Rev. C **76**, 014315 (2007).

[10] T. Dytrych, K. D. Launey, J. P. Draayer, P. Maris, J. P. Vary, E. Saule, U. Catalyurek, M. Sosonkina, D. Langr and M. A. Caprio, Phys. Rev. Lett. **111**, 252501 (2013).

[11] C. W. Johnson, Phys. Rev. C **91**, 034313 (2015).

[12] A. E. McCoy, M. A. Caprio and T. Dytrych, Ann. Acad. Rom. Sci. Ser. Chem. Phys. Sci. **3**, 17 (2018).

[13] Y. Kanada-En'yo, M. Kimura and A. Ono, Prog. Exp. Theor. Phys. **2012**, 01A202 (2012).

[14] B. R. Barrett, P. Navrátil and J. P. Vary, Prog. Part. Nucl. Phys. **69**, 131 (2013).

[15] M. A. Caprio, P. Maris and J. P. Vary, Phys. Lett. B **719**, 179 (2013).

[16] P. Maris, M. A. Caprio and J. P. Vary, Phys. Rev. C **91**, 014310 (2015); Erratum: *ibid.* **99**, 029902(E) (2019).

[17] M. A. Caprio, P. Maris, J. P. Vary and R. Smith, Int. J. Mod. Phys. E **24**, 1541002 (2015).

[18] A. M. Shirokov, J. P. Vary, A. I. Mazur and T. A. Weber, Phys. Lett. B **644**, 33 (2007).

[19] A. M. Shirokov, I. J. Shin, Y. Kim, M. Sosonkina, P. Maris and J. P. Vary, Phys. Lett. B **761**, 87 (2016).

[20] P. Maris, M. Sosonkina, J. P. Vary, E. Ng and C. Yang, Procedia Comput. Sci. **1**, 97 (2010).

[21] H. M. Aktulga, C. Yang, E. G. Ng, P. Maris and J. P. Vary, Concurrency Computat.: Pract. Exper. **26**, 2631 (2014).

[22] M. Shao, H. M. Aktulga, C. Yang, E. G. Ng, P. Maris and J. P. Vary, Comput. Phys. Commun. **222**, 1 (2018).

[23] P. Ring and P. Schuck, *The nuclear many-body problem.* Springer-Verlag, New York, 1980.

[24] D. J. Rowe, *Nuclear collective motion: Models and theory.* World Scientific, Singapore, 2010.

[25] J. Kelley, E. Kwan, J. E. Purcell, C. G. Sheu and H. R. Weller, Nucl. Phys. A **880**, 88 (2012).

[26] C. Forssen, J. P. Vary, E. Caurier and P. Navratil, Phys. Rev. C **77**, 024301 (2008).

[27] P. Maris, J. P. Vary and A. M. Shirokov, Phys. Rev. C **79**, 014308 (2009).

[28] D. R. Entem and R. Machleidt, Phys. Rev. C **68**, 041001 (2003).

[29] P. Maris, M. A. Caprio and J. P. Vary, Phys. Rev. C **91**, 014310 (2015).

[30] H. G. Bohlen, W. von Oertzen, R. Kalpakchieva, T. N. Massey, T. Corsch, M. Milin, C. Schulz, Tz. Kokalova and C. Wheldon, J. Phys. Conf. Ser. **111**, 012021 (2008).

[31] G.-B. Liu and H. T. Fortune, Phys. Rev. C **42**, 167 (1990).

[32] Y. Hirayama, T. Shimoda, H. Izumi, A. Hatakeyama, K. P. Jackson, C. D. P. Levy, H. Miyatake, M. Yagi and H. Yanoa, Phys. Lett. B **611**, 239 (2005).

[33] N. Fukuda *et al.*, Phys. Rev. C **70**, 054606 (2004).

[34] H. G. Bohlen *et al.*, Nucl. Phys. A **722**, 3c (2003).